Biogeosciences Discuss., 11, 11747–11783, 2014
www.biogeosciences-discuss.net/11/11747/2014/
doi:10.5194/bgd-11-11747-2014

Biogeosciences Discussions
Open Access

Intercomparison of fast response commercial gas analysers for nitrous oxide flux measurements under field conditions

Ü. Rannik[1], S. Haapanala[1], N. J. Shurpali[2], I. Mammarella[1], S. Lind[2], N. Hyvönen[2], O. Peltola[1], M. Zahniser[3], P. J. Martikainen[2], and T. Vesala[1]

[1]Department of Physics, P.O. Box 48, 00014 University of Helsinki, Finland
[2]Department of Environmental Science, University of Eastern Finland, Kuopio, Finland
[3]Center for Atmospheric and Environmental Chemistry, Aerodyne Research Inc., Billerica MA, USA

Received: 19 May 2014 – Accepted: 12 July 2014 – Published: 1 August 2014

Correspondence to: Ü. Rannik (ullar.rannik@heuristica.ee)

Published by Copernicus Publications on behalf of the European Geosciences Union.

Abstract

Four gas analysers capable of measuring nitrous oxide (N_2O) concentration at a response time necessary for eddy covariance flux measurements were operated from spring till winter 2011 over a field cultivated with reed canary grass (RCG, *Phalaris arundinaceae*, L.), a perennial bioenergy crop in Eastern Finland. The instruments were TGA100A (Campbell Scientific Inc.), CW-TILDAS-CS (Aerodyne Research Inc.), N2O/CO-23d (Los Gatos Research Inc.) and QC-TILDAS-76-CS (Aerodyne Research Inc.). The period with high emission, lasting for about two weeks after fertilization in late May, was characterised by an up to two orders of magnitude higher emission, whereas during the rest of the campaign the N_2O fluxes were small, from 0.1 to 1 nmol m^{-2} s^{-1}. Two instruments, CW-TILDAS-CS and N2O/CO-23d, determined the N_2O exchange with minor systematic difference throughout the campaign, when operated simultaneously. TGA100A produced cumulatively highest N_2O estimates (with 29 % higher value during the period when all instruments were operational). QC-TILDAS-76-CS obtained 36 % lower fluxes than CW-TILDAS-CS during the first period, including the emission episode, whereas the correspondence with other instruments during the rest of the campaign was good. The reason for these episodic higher and lower estimates by the two instruments is not currently known, suggesting further need for detailed evaluation of instrument performance under field conditions with emphasis on stability, calibration and, in particular, simultaneous accurate determination of water vapour concentration due to its large impact on small N_2O fluxes through spectroscopic and dilution corrections. The instrument CW-TILDAS-CS was characterised by the lowest noise level (std around 0.12 ppb at 10 Hz sampling rate), as compared to N2O/CO-23d and QC-TILDAS-76-CS (around 0.50 ppb) and TGA100A (around 2 ppb). Both instruments based on Continuous-Wave Quantum Cascade Lasers, CW-TILDAS-CS and N2O/CO-23d, were able to determine the same sample of low N_2O fluxes with high mutual coefficient of determination at 30 min averaging level and with minor systematic difference over the observation period of several months.

BGD
11, 11747–11783, 2014

1 Introduction

During the last years there has been a rapid development in the application of laser spectroscopy for greenhouse gas measurements. In particular, development of fast response N_2O analyzers based on spectroscopic techniques (e.g. tunable diode laser (TDL) and quantum cascade laser (QCL) spectrometers) has facilitated the eddy covariance (EC) measurements of N_2O exchange in different ecosystems. Such measurements have been reported in literature and they have been carried out in different ecosystems such as agricultural (Smith et al., 1994; Wienhold et al., 1994; Christensen et al., 1996; Laville et al., 1997; Scanlon and Kiely, 2003; Neftel et al., 2007; Kroon et al., 2007), forest (Pihlatie et al., 2005; Eugster et al., 2007) as well over urban canopies (Famulari et al., 2010; Järvi et al., 2014).

The observed N_2O emissions are episodic in nature, showing high spatial and temporal variability. Emission bursts of short duration, typically occurring after fertilizer application, or associated with thawing and rain events (Kroon et al., 2007; Pihlatie et al., 2010), are followed by long periods of small fluxes, when also uptake of N_2O has been observed (Flechard et al., 2005). Overall, N_2O fluxes reported by previous studies are characterised by large uncertainty and temporal variability, which are related to biogeochemical soil processes and several systematic and random error sources of the EC measurements. One of the sources of uncertainty for the N_2O fluxes measured by the EC technique is the performance and stability of fast response gas analyzers. Some studies performed under field conditions (Eugster et al., 2007; Kroon et al., 2007; Neftel et al., 2009) have reported that the laser drift can cause occasional over- or underestimation of EC flux. The instrumental drift typically characterizes TDL as well as QCL spectrometers (Werle et al., 1993; Nelson et al., 2002). Mammarella et al. (2010) thoroughly investigated the performance of TDL instruments in measurements of N_2O fluxes by the EC technique. They suggested that high pass filtering could be used to remove the low-frequency signal drifting, which could otherwise contaminate the detected concentration time series and significantly increase the flux uncertainty.

BGD
11, 11747–11783, 2014

Apart from the episodic emissions, N_2O fluxes are typically small in magnitude (in the order of one to one hundred $\mu g\,N\,m^{-2}\,h^{-1}$, which corresponds to N_2O flux range from 10^{-2} to 1 $nmol\,m^{-2}\,s^{-1}$ as presented in the units used in the current study), being on the detection limit of the EC systems (e.g. Pihlatie et al., 2005; Wang et al., 2013). Small fluxes imply small turbulent fluctuations of the concentration, requiring high precision of the instruments to be able to resolve those fluctuations. In other words, the signal (turbulent fluctuations) to instrumental noise ratio has to be high enough to achieve sufficiently low flux error arising due to the noise present in measured signals (Lenschow and Kristensen, 1985).

The goals of this study are to compare the available equipment for N_2O flux measurements employing the EC technique and to evaluate their performance, ability to detect small fluxes and long-term stability in determining the N_2O exchange. The instruments used were TGA100A (Campbell Scientific Inc.), CW-TILDAS-CS (Aerodyne Research Inc.), N2O/CO-23d (Los Gatos Research Inc.) and QC-TILDAS-76-CS (Aerodyne Research Inc.), which shall be further referred to as CS-TDL, AR-CW-QCL, LGR-CW-QCL and AR-P-QCL, respectively, throughout this study by using the combinations of acronyms for manufacturer and the laser type (see Table 1). In addition, the methods for flux calculation using the laser spectrometer data are evaluated and the magnitude and dynamics of N_2O fluxes during the RCG growing season are determined.

2 Materials and methods

2.1 Site

The measurement site was a 6.9 ha field cultivated with RCG, a perennial bioenergy crop. The site was located on the rural area of Maaninka, Eastern Finland (63°9′48.69″ N, 27°14′3.29″ E). Long-term (reference period 1981–2010; Pirinen et al., 2012) annual air temperature in the region is 3.2 °C, the coldest month of the year is February and the warmest is July, with monthly mean air temperature being −9.4 °C

BGD
11, 11747–11783, 2014

and 17.0 °C, respectively. The annual precipitation in the region is 612 mm. Part of this precipitation amount falls as snow. Snow cover season starts in October and lasts until the end of April with a maximum snow cover of approximately 50 cm. The RCG crop at the Maaninka site was fertilized in the beginning of the growing season (late May), resulting in a large emission pulse of N_2O. The canopy height developed throughout the growing season from about 10 cm in mid-May to 1.7 m by late June. The increase in plant height was almost linear in time between these periods and starting from July changed slowly up to 1.9 m.

The soil at the study site is classified as fine sand to coarse silt (particle size 0.03–0.06 mm). According to the World Reference Base for Soil Resources (WRB) system (FAO, 2006), the soil is classified as Regosol. The soil pH varies from 5.4 to 6.1 within the ploughing depth from the surface to about 30 cm, electrical conductivity between 960 to 3060 $\mu S\,cm^{-1}$ and soil organic matter content between 3 and 11 %. The average C/N ratio in the ploughing depth is 14.9 (ranging from 14.1 to 15.7). The soil particle density is about 2.65 $g\,cm^{-3}$ within the soil depth from the surface to about 20 cm.

2.2 Measurements

Measurements were conducted by the University of Helsinki (UH) and by the University of Eastern Finland (UEF), operating separate EC systems. The UH measurement setup included a 3-D ultrasonic anemometer (USA-1, METEK GmbH, Elmshorn, Germany) to acquire the wind components. The anemometer was installed on top of a pole, the measurement height being 2.2 m. The measurement height was raised to 2.4 m on 30 June 2011 due to the RCG growth. Gas analyzers were situated in an air conditioned cabin located about 15 m east from the anemometer pole. This wind direction (50–110° sector) was therefore discarded from further analysis due to possible disturbances to flux measurements. Sample inlets for gas analyzers were located 10 cm below the anemometer. The N_2O instruments operated by the UH were the instrument based on tunable diode laser CS-TDL (model TGA100A, Campbell Scientific Inc.), and two instruments based on continuous wave quantum cascade lasers, AR-CW-QCL (models

BGD
11, 11747–11783, 2014

CW-TILDAS-CS, Aerodyne Research Inc., see e.g. Zahniser et al., 2009; Lee et al., 2011) and LGR-CW-QCL (model N2O/CO-23d, Los Gatos Research Inc., see e.g. Provencal et al., 2005). Sampling lines of AR-CW-QCL and LGR-CW-QCL were heated slightly above ambient temperature in order to avoid water from condensing to the lines. CS-TDL had a dryer just before the instrument and no sampling line heating was used. Further details of the involved instruments are given in Table 1 and details of the different setups are given in Table 2.

The maintenance of CS-TDL was the most demanding of the compared instruments. It uses liquid nitrogen to keep the laser source at the operating temperature, and the Dewar was filled up twice a week. The operating parameters of the analyser, such as laser current and laser and detector temperatures were checked once a week and after power failures. In addition, the inlet filter of CS-TDL was changed once a month.

The operating parameters of AR-CW-QCL were fine-tuned at the site after instrument installation. The instrument manufacturer provided a software upgrade during the campaign to conduct the real-time water vapour correction to the trace gas concentration data analysed by the instrument. In addition, the operating parameters were fine-tuned a few times on-line by the instrument manufacturer during the campaign.

LGR-CW-QCL arrived in the campaign later (see Sect. 3 for details). After about two weeks of operation, the laser drifted out of the tuning range and the laser offset current was tuned manually to enable correct operation again.

The UEF set up included a pulsed quantum cascade laser spectrometer AR-P-QCL (Model QC-TILDAS-76-CS, Aerodyne Research Inc., Billerica, MS, USA, see McManus et al., 2005), an infrared gas analyser (IRGA, Model Li-6262) and a 3-D sonic anemometer (Model R3-50, Gill Instruments, Ltd., Hampshire, UK) for fast response gas concentration and wind component measurements (Tables 1 and 2). The heated intake tubes for the laser spectrometer and IRGA were installed on either sides of the sonic anemometer, all mounted on a boom on an adjustable instrument mast. The mast height was set at 2.0 m above the soil surface in the beginning of the campaign. To adjust to the increasing plant height, the mast was raised to 2.5 m during mid-June.

BGD
11, 11747–11783, 2014

AR-P-QCL was set up to measure simultaneously the N_2O, CO_2 and water vapour mixing ratios, while the IRGA was used to monitor the CO_2 and water vapour mixing ratios. Both trace gas analysers were calibrated against standard gases minimum once a month during the campaign, in particular AR-P-QCL was calibrated every 2–3 weeks during summer with two standard gases 299 and 342 ppb.

A weather station set up on another mast close to the EC mast monitored the supporting meteorological variables. The weather station mast height was also adjusted according to the changes in EC mast height. Supporting measurements included air temperature and relative humidity (Model: HMP45C, Vaisala Inc.) using radiation shield, atmospheric pressure (Model CS106 Vaisala PTB110 Barometer), wind speed and direction (Model 03002-5, R.M. Young Company) and several other variables not used in current study. Data was collected using a datalogger (model CR 3000, Campbell Scientific Inc.). Except air pressure (stored as hourly averages), meteorological data was stored as 30 min averages. Short gaps in the data were filled using linear interpolation, but when air temperature, relative humidity, pressure or rainfall data were missing for longer periods, data from Maaninka weather station operated by the Finnish Meteorological Institute located about 6 km to South-East from the site, was used.

2.3 Flux processing

Measurements were sampled at 10 Hz frequency. Filtering to eliminate spikes was performed according to standard approach (Vickers and Mahrt, 1997), where the high frequency eddy covariance data were despiked by comparing two adjacent measurements. If the difference between two adjacent concentration measurements of N_2O was greater than 20 ppb, the following point was replaced with the same value as the previous point.

The spectroscopic correction due to water vapour impact on the absorption line shape was applied along with Webb–Pearman–Leuning (WPL) dilution correction due to water vapour on high-frequency raw concentration output X_C (mixing ratio with re-

BGD
11, 11747–11783, 2014

spect to moist air, uncorrected for spectroscopic effect) according to $\chi_C = \frac{\chi_C}{1-(1+b)\chi_V}$, where χ_C and χ_V are the instantaneous mixing ratios of N_2O and water vapour with respect to the dry air and b is the spectroscopic correction coefficient determined experimentally for each instrument (Table 1) by measuring the response of instrument (output χ_C) on sample air of standard gas (constant χ_C) with varying water content χ_V. The correction was not necessary for CS-TDL as a dryer installed after the air intake point on the sampling line dried the air sample before the optical cell. LGR-CW-QCL corrected for the water vapour effect by a built-in module in the LGR data acquisition software.

Prior to calculating the turbulent fluxes, a 2-D rotation (mean lateral and vertical wind equal to zero) of sonic anemometer wind components was done according to Kaimal and Finnigan (1994) and all variables were linearly detrended. The EC fluxes were calculated as 30 min co-variances between the scalars and vertical wind velocity following commonly accepted procedures (e.g. Aubinet et al., 2000). Time lag between the concentration and wind measurements induced by the sampling lines was determined by maximizing the covariance. For CS-TDL the lag was determined by maximizing the covariance for high flux period only (day of year (DOY) 144-146) because in other periods the lag was not well defined by using this method. The final processing (instruments CS-TDL, AR-CW-QCL and LGR-CW-QCL) was done by fixing the time lag to avoid unphysical variation of lag occurring due to random flux errors. For AR-P-QCL system the lag was determined by maximising the covariance for CO_2 and the same lag was assigned to N_2O. This was to use the advantage that the instrument measured also CO_2 and therefore enabled to use much better signal-to-noise ratio in determination of the lag time. Spectral corrections were applied to account for the low and high frequency attenuation of the co-variances (Sect. 2.4). Then, the humidity effect on temperature flux was accounted for after Schotanus et al. (1983). All data processing was performed with post-processing software EddyUH (http://www.atm.helsinki.fi/Eddy_Covariance/EddyUHsoftware.php).

BGD
11, 11747–11783, 2014

2.4 Spectral corrections

Low and high frequency variations in the measured signal are attenuated due to data acquisition and processing, and by a non-ideal measurement system (e.g. Moore, 1986; Moncrieff et al., 1997; Rannik and Vesala, 1999; Massman, 2000). Block averaging and detrending of data acts as a high pass filter, thus damping low frequency fluctuations (Rannik and Vesala, 1999; Finnigan et al., 2003). Turbulent fluctuations occurring at high frequencies are attenuated due to the measurement system's limitations. Gas analyzer's finite frequency response, attenuation of fluctuations in the sampling line, spatial separation between the anemometer measurement head and sampling line inlet affect the attenuation of high frequency fluctuations in the signal.

The observed flux (F_m) can be formally presented as the integral over multiplication of the true co-spectrum (Co, unaffected by frequency attenuation) with the co-spectral transfer function as

$$F_m = \int_0^\infty T(f)\mathrm{Co}(f)\mathrm{d}f, \quad (1)$$

where the co-spectral transfer function can be presented as the multiplication of respective low-frequency $T_L(f)$ and high-frequency $T_H(f)$ transfer functions. For the low-frequency transfer functions due to high-pass filtering and/or finite averaging period see Rannik and Vesala (1999).

For evaluation of the instrument frequency performance and subsequent high-frequency flux corrections during post-processing, the high-frequency transfer function of the EC-system was estimated (Aubinet et al., 2000) as the ratio of the observed and not-attenuated flux (Horst, 1997). The co-spectral transfer function $T_H(f)$ of an EC system for a system behaving as a first order response sensor can be described by

$$T_H(f) = \frac{1}{1 + (2\pi f\tau)^2}, \quad (2)$$

BGD
11, 11747–11783, 2014

where f is the natural frequency and τ the (first order) response time of the attenuator (sensor or the system in total) (Horst, 1997). The effective transfer function of the EC system for different instruments was estimated as the ratio of co-spectral density of scalar flux relative to co-spectrum of sensible heat flux (Aubinet et al., 2000). Such a procedure assumed that temperature measurements were not affected by attenuation (true for the sonic anemometer) and includes normalisation with integral over frequencies not affected by attenuation.

2.5 Estimation of random errors

Turbulent fluxes averaged over a limited time period have random errors because of the stochastic nature of turbulence (Lenschow et al., 1994; Rannik et al., 2006) as well as due to noise presented in measured signals (Lenschow and Kristensen, 1985).

The random error of the covariance can be evaluated as the standard deviation of the co-variance, hereafter in the manuscript denoted by δ_F. Theoretically, there are several ways to approximate the same error estimate. Currently, the standard deviation of the co-variances was calculated according to method implemented in EddyUH, e.g. the one proposed by Finkelstein and Sims (2001). The method evaluates the error in time domain through integration of the auto-covariance and cross-covariance functions of the vertical wind speed and the scalar concentration. This mathematically rigorous method provides estimates for the random uncertainty of the flux measurements for every averaging period.

Random uncertainty of the observed co-variance due to presence of noise in instruments signal, giving essentially the detection limit of the flux that the system is able to measure, can be expressed in its simplest form as

$$\delta_{\mathrm{F,noise}} = \frac{\sigma_{\mathrm{w}}\sigma_{\mathrm{noise}}}{\sqrt{fT}}, \tag{3}$$

where σ_{w} and σ_{noise} denote the standard deviation of the turbulent record of vertical wind speed and the standard deviation of instrumental noise as observed at frequency

BGD
11, 11747–11783, 2014

f, T denotes the flux averaging period. The expression above assumes that the noise component of the vertical wind speed measurement is negligible. In this study we use the method developed by Lenschow et al. (2000) and applied to EC fluxes by Mauder et al. (2013) to estimate the flux detection limit due to instrumental noise. Lenschow et al. (2000) derived the method to estimate the instrumental random noise variance σ_{noise} from the auto-correlation function of the measured turbulent record close to zero-shift and enables to determine the flux detection limit for each half-hour flux averaging period.

If an average over fluxes F_i $(i = 1, \ldots, N)$ is calculated, each of these representing a flux value observed over averaging period T and being characterised by an error $\delta_{\text{F},i}$, then the error of the average flux $\langle F \rangle = \frac{1}{N} \sum_{i=1}^{N} F_i$ can be expressed as

$$\Delta_{\langle F \rangle} = \sqrt{\frac{\sum_{i=1}^{N} (\delta_{\text{F},i})^2}{N^2}}. \quad (4)$$

This expression will be used to estimate the random errors of the average fluxes in Sect. 3.4.

3 Results

The intercomparison measurements were performed from the beginning of the growing season in April till November 2011. According to instrumental data coverage, the period was divided into three sub-periods for the instrument evaluation and flux analysis purposes. During the period I, DOY 110-181 (20 April–30 June 2011), the measurements of CS-TDL, AR-CW-QCL and AR-P-QCL were available, during the period II, DOY 206-271 (25 July–28 September 2011), all instruments were measuring and during period III, DOY 272–324 (29 September–20 November 2011), all other except CS-TDL were operational. Prior to analysis data quality screening was performed. The measurements corresponding to wind direction interval 50–110° were excluded as possibly

BGD
11, 11747–11783, 2014

affected by instrumental cabin. In addition, quality screening was performed according to Vickers and Mahrt (1997) by applying the following statistics and selection thresholds: data with N_2O concentration skewness outside (−2,2), or kurtosis outside (1, 8), or Haar mean and Haar variance exceeding 3 were rejected. Applying the same statistics and thresholds as for N_2O, additional quality screening was performed according to H_2O concentration statistics for LGR-CW-QCL and AR-P-QCL due to the impact of the spectroscopic and dilution corrections on fluxes and according to CO_2 concentration statistics for AR-P-QCL because the lag obtained for CO_2 was assigned to N_2O in case of this instrument.

The fluxes obtained for three periods are presented in Fig. 1, being averaged over daily period for the clarity of presentation. No gap-filling was used and for each day only the existing measurements, after applying data quality screening described above, were averaged. In May the fluxes increased significantly after the fertilization and then decreased back to low, although clearly positive level after a few weeks. This was the only occasion of high N_2O emission followed by continuous decrease of fluxes towards the autumn. The high fluxes observed during that period enabled to evaluate the frequency performance of three systems including CS-TDL, AR-CW-QCL and AR-P-QCL. The LGR-CW-QCL instrument was not operational then and the frequency response for this instrument was performed based on the concurrently measured H_2O and CO signal analysis.

3.1 Spectral characteristics of instruments

Spectral analysis was performed to study the frequency performance of the instruments. For the period 26 May, from 07:00 to 13:00 EET (Eastern European Time) when the conditions corresponded to moderately unstable (average wind speed of the period $3.2\,m\,s^{-1}$ and sensible heat flux $50\,W\,m^{-2}$), the calculated spectra exhibited very clear and systematic patterns for temperature as well as N_2O concentration records measured by three instruments (Fig. 2). In spite of high fluxes registered by the instruments during this period, CS-TDL N_2O signal was dominated by noise almost over the whole

BGD
11, 11747–11783, 2014

frequency range presented. For AR-CW-QCL, almost no evidence of noise could be observed in the power spectral plot (multiplied with frequency). The older version by Aerodyne, the AR-P-QCL instrument, revealed increase of the spectral density only at the high-frequency end of the power spectrum, being characteristic to some noise contribution. The co-spectra of all three instruments showed smooth patterns, the shape being consistent with the co-spectral model by Kaimal et al. (1972) but slightly shifted in frequency scale. At the high frequency ends of the presented co-spectra the N_2O signal curves deviate from the theoretical as well as from temperature co-spectra, indicating attenuation of signals at high frequencies by the measurement systems.

The same time period was used to estimate the frequency response of the N_2O eddy covariance systems according to method described in Sect. 2.4 (Fig. 3). The time constants estimated by making use of co-spectra presented in Fig. 2 and eq. (2) for CS-TDL, AR-CW-QCL and AR-P-QCL were 0.12, 0.07 and 0.08 s, respectively. Note that these time constants characterise the frequency response of the systems in total.

Although the response time obtained for AR-P-QCL system from high flux period was 0.08 s, the analysis of the response time from measured CO_2 signal for several other periods yielded the average response time 0.15 s. The average higher value could result from syncronisation of N_2O signal according to the lag determined for CO_2 flux and hence we choose the constant value 0.15 s for co-spectral corrections throughout the campaign for this instrument.

Spectral analysis was performed also for the period when LGR-CW-QCL measurements were available. For the comparison purposes, the results for a time period in 4 August form 00:30 to 04:00 EET (Eastern European Time) are presented for AR-CW-QCL and LGR-CW-QCL instruments (Fig. 4). The period was chosen with relatively high fluxes (with LGR-CW-QCL measurements available) and similar stability and wind conditions (average wind speed of the period 0.94 m s^{-1} and sensible heat flux -37.5 W m^{-2}). The power spectra of both instruments revealed contribution of noise at high frequency ends of the spectra, being more pronounced for LGR-CW-QCL. The co-spectra were more scattered when compared to high flux period (Fig. 2). Estimation

BGD
11, 11747–11783, 2014

of the frequency response of the systems based on this period was uncertain due to scatter and could not be used as the basis for co-spectral corrections for LGR-CW-QCL.

The main difference in the flow setups of the systems concerned LGR-CW-QCL. With larger tube diameter and slightly lower flow rate the flow regime was likely laminar ($Re \approx 2000$), whereas for other instruments it was clearly turbulent ($Re \approx 4600$). It is well established that under laminar flow regime tube flow attenuates turbulent fluctuations of concentrations much more than under turbulent flow. According to expression for tube attenuation in laminar flow regime (Foken et al., 2012) the first order response time for LGR-CW-QCL flow setup would be 0.37 s (estimated for N_2O). For turbulent flow (ARI-CW-QCL setup) the theoretical response time for tube damping is much smaller (0.01 s) than the response time obtained from the co-spectra (0.07 s), suggesting that the system's response was dominated by the instrumental response.

The frequency response of the LGR-CW-QCL system was further determined from the co-spectral analysis of the CO signal and we obtained the value 0.26 s. We determined also the experimental response time for water vapour from several periods and we consistently found the value around 0.35 s (for LGR-CW-QCL system). For comparison, the response time for ARI-CW-QCL system was determined to be 0.10 s. Damping of water fluctuations in sampling line is stronger than for other scalars as evidenced by experimental studies (e.g. Mammarella et al., 2009). This is due to adsorption/desorption of water molecules on tube walls. This explains the difference between the response times obtained from CO and H_2O. Thus we believe that a value of 0.26 s characterises well the first order response time of LGR-CW-QCL setup for N_2O and we use this value in co-spectral corrections. Note, however, that a higher frequency response time of the LGR-CW-QCL system does not mean a slower instrument performance because the system has more damping primarily in sampling line due to lower flow rate and larger tube diameter (Table 2).

BGD
11, 11747–11783, 2014

The frequency response times determined in this section were used in performing the co-spectral corrections (Table 2) as described in Sect. 2.4, typical magnitudes of these corrections are presented in Table 3.

3.2 Random uncertainty of fluxes and instrumental noise

The method by Lenschow et al. (2000) described in Sect. 2.5 enables us to calculate the instrumental noise for each 30 min period and the resulting flux uncertainty due to instrumental noise. Figure 5a shows the estimated signal noise statistics with upper and lower percentiles and quantiles (boxes) with a median value in the middle. For all instruments except LGR-CW-QCL the distributions are very narrow and different percentiles cannot be separated from the plot (for values see Table 1). This tells us that the noise levels of the three instruments are very stable, but the noise level of LGR-CW-QCL somewhat varies. In comparison of the instruments, AR-CW-QCL has by far the lowest noise level of around 0.12 ppb (standard deviation of the signal noise at 10 Hz frequency). The two instruments, LGR-CW-QCL and AR-P-QCL, are characterised by a similar noise level (around 0.5 ppb), while CS-TDL signals show the highest noise level (2 ppb). Consequently, these instrumental noise levels are reflected in the random errors of fluxes, determining essentially the minimum flux level that each instrument is able to measure at a given flux averaging interval (30 min period). For AR-CW-QCL the respective flux detection limit is around 10^{-2} nmol m^{-2} s^{-1} (as given by median in Fig. 5b), for LGR-CW-QCL and AR-P-QCL around 4×10^{-2} nmol m^{-2} s^{-1} and for CS-TDL 0.15 nmol m^{-2} s^{-1}. Note that these values depend also on observation conditions via the standard deviation of vertical wind speed σ_w, as expressed by Eq. (3).

The frequency distributions of the total flux random errors, calculated according to Finkelstein and Sims (2001) as described in Sect. 2.5, are naturally higher than the flux error due to instrumental noise only. It can be observed that in case of full flux random error the difference between different instruments is reduced (Fig. 5b) because in addition to instrumental noise impact this error statistic also incorporates the flux uncertainty due to stochastic nature of turbulence. The relative random errors (Fig. 5c)

BGD
11, 11747–11783, 2014

are the largest for CS-TDL (being in the order of 100 % and in most cases less than ±300 %) and the smallest for AR-CW-QCL (median around 30 % and mostly the error being less than 100 %) instruments. It is the signal noise of the instrument that contributes to the random error of the flux, determining which instrument is able to detect lowest fluxes. In the case of CS-TDL the low-frequency signal drifting, characteristic of this instrument (see for more details Mammarella et al., 2010), also can enlarge the total random error of the calculated flux.

3.3 Intercomparison of fluxes averaged over turbulent spectrum

It was observed that the fluxes calculated from CS-TDL measurements during the low flux period were dominated by random uncertainty, being frequently in the order of the minimum detectable flux values (Sect. 3.2). Therefore, the fluxes averaged over 30 min period were compared for this instrument with AR-CW-QCL results over the period DOY 110–182, which included the high emission episode starting from DOY 144 and exhibiting elevated fluxes until approximately DOY 155. In general the fluxes with high magnitude obtained by CS-TDL compared well with those of obtained by AR-CW-QCL (Fig. 6a). At around zero fluxes as measured by AR-CW-QCL, the results by CS-TDL showed scattered values roughly between ±5 nmol m^{-2} s^{-1}. This is consistent with the high flux detection limits as described in the previous section. The AR-P-QCL system, as compared with AR-CW-QCL, showed systematically lower fluxes during the given period of high fluxes (slope 0.70). In spite of lower noise level of this instrument, the coefficient of determination for this instrument (0.63) was lower than that for CS-TDL (0.77) in comparison to the fluxes as measured by AR-CW-QCL. Note that during the second observation period, when fluxes were much lower, CS-TDL was not able to determine fluxes with sufficiently small error and the correlation with AR-CW-QCL at 30 min averaging level was very low (Fig. 6c).

The comparison of the 30 min average fluxes calculated from two instruments, AR-CW-QCL and LGR-CW-QCL, revealed very good correspondence and high correlation (R^2 = 0.90) even though those measurements corresponded to much lower N_2O fluxes.

BGD
11, 11747–11783, 2014

The slope close to unity and negligible intercept indicates no systematic bias between the measurements of these systems (Fig. 6d).

3.4 Long-term averages and systematic differences

In order to evaluate the possible systematic differences, cumulative curves of the flux observations were calculated. No gap-filling of missing data was done but instead only the half-hour periods were used when the results for all instruments were available. Thus the cumulative sums do not assume representing the total emissions over the given periods, although rough estimates could be calculated by accounting in total sums with the data coverage percentage presented in Table 4. The summation of fluxes over the first and second periods reveals that CS-TDL gives the highest flux sums and AR-P-QCL the lowest, in particular during the first period (Fig. 7). The cumulative sums for fluxes obtained from AR-CW-QCL and LGR-CW-QCL measurements converge over 2nd and 3rd periods and show only small differences. Also the cumulative fluxes measured by AR-P-QCL during these periods are very close to fluxes measured by the two other instruments. In order to assess the magnitude of the random errors in these differences, the random errors of the fluxes averaged over three periods were calculated according to Eq. (4). The analysis revealed that the average fluxes for period II, obtained from the measurements of AR-CW-QCL and LGR-CW-QCL instruments did not differ within calculated error limits, and were very close during the period III with the result for AR-P-QCL (Table 4).

However, CS-TDL produced a 7 % higher total sum for the period of high fluxes (DOY 110–181 with an average flux of 0.87 nmol m^{-2} s^{-1} as determined by AR-CW-QCL) and a 29.0 % higher sum for the second period (DOY 206–271) compared to an average flux 0.142 nmol m^{-2} s^{-1} (average of AR-CW-QCL and LGR-CW-QCL results). The AR-P-QCL instrument determined for these two periods 36 % and 13 % lower average fluxes, respectively. The possible reasons for this will be discussed in the next section. For the third period, the results for AR-P-QCL did not differ much from the results of the other two instruments.

BGD
11, 11747–11783, 2014

4 Discussion and conclusions

Performance of four instruments capable of fast response measurement of N_2O was studied throughout the 2011 growing season over a field cultivated with RCG in Eastern Finland. The instruments used in the EC systems were TGA100A by Campbell Scientific Inc. (CS-TDL), CW-TILDAS-CS by Aerodyne Research Inc. (AR-CW-QCL), N2O/CO-23d by Los Gatos Research Inc. (LGR-CW-QCL) and QC-TILDAS-76-CS by Aerodyne Research Inc. (AR-P-QCL). The N_2O fluxes were small in the beginning of the season, increased significantly after the fertilization (late May) and then decreased back to low, positive values after a few weeks. Three instruments, CS-TDL, AR-CW-QCL and AR-P-QCL were operational during this high emission period. During this period, all instruments detected the same flux dynamics, whereas the fluxes obtained from the older instrument by Aerodyne, AR-P-QCL, were lower compared to the other two instruments.

After the high emission period, when the N_2O fluxes were small, they were mostly below the flux detection limit for CS-TDL. When it was operational, the cumulative emission estimate over the period was 29 % higher than the average result for instruments based on the continuous wave quantum cascade lasers, AR-CW-QCL and LGR-CW-QCL. The two CW-QCL instruments compared very well on half-hour basis as well as produced statistically close cumulative fluxes over the period when the two instruments were simultaneously operational (25 July 2011–20 November 2011). This enabled us to make an indirect conclusion that the spectroscopic and water vapour dilution corrections for AR-CW-QCL and LGR-CW-QCL were adequate. Note that those corrections were done by built in functionality in case of LGR-CW-QCL and in post processing phase for AR-CW-QCL.

CS-TDL differs from the other instruments used in the inter-comparison study by its design and has been characterised by signal drifting (Mammarella et al., 2010). The signal drifting makes the time series produced by the instrument essentially non-stationary and therefore enhances the random variability of the flux estimate around the

BGD
11, 11747–11783, 2014

true value. However, such enhanced random uncertainty should not affect systematically the cumulative sums over longer periods. Therefore the systematically higher flux estimates during the second period can potentially be the result of calibration and/or limited stability of the system over time.

The instrument by Aerodyne ARI-P-QCL is based on the pulsed quantum cascade laser. For this instrument the experimentally determined spectroscopic correction coefficient was much lower than the coefficient for AR-CW-QCL (Table 1). The reason for systematically lower values of fluxes determined by AR-P-QCL from the beginning of the experiment in April till June 2011, but subsequent relatively good comparison with other instruments till the end of the experiment in November 2011, is not known. Two types of corrections were applied to N_2O fluxes: the spectroscopic correction to account for the impact of water vapour on the absorption line shape, and the co-spectral correction. The latter correction was comparable to all instruments (Table 3) and does not introduce significant difference between instruments. The spectroscopic correction was applied together with the water vapour dilution correction (Sect. 2.3) and can constitute a major correction depending on the value of the coefficient b. The correction is related to the water vapour flux, which was during the day time on the average around 100 W m^{-2} (periods I and II, Table 5), with mid-day averages around 150 to 200 W m^{-2}. Considering the average concentration of N_2O around 330 ppb and the spectroscopic correction value b = 0.39 (the value for AR-CW-QCL), the spectroscopic correction can be a few tenths of nmol m^{-2} s^{-1} during mid-day, which is of the order of the flux magnitude. We do not however have any reasons to suspect that the spectroscopic correction coefficient value for AR-P-QCL was inaccurately determined and larger spectroscopic correction would not explain systematic difference observed during the first period only. Thus the reasons for flux underestimation by AR-P-QCL during the period I are not known and we suggest that extreme care should be exercised during the long-term measurement campaigns both with N_2O and H_2O calibrations due to the strong impact of the latter on the N_2O flux through spectroscopic and dilution corrections.

BGD
11, 11747–11783, 2014

At half-hour averaging time scale, the flux estimates for AR-CW-QCL and LGR-CW-QCL instruments were very well correlated and showed good correspondence. Apart from high N_2O fluxes exceeding a few nmol m^{-2} s^{-1} during the high emission period, CS-TDL was not able to resolve the emission fluxes at half-hourly time scale. Therefore one can conclude that CS-TDL is not suitable for measuring such low fluxes if the aim is to resolve fluxes at hourly time scale and not simply the daily averages.

Important characteristics of the instruments for performing the EC measurements are the response time and the noise level. The response times for CS-TDL, AR-CW-QCL and AR-P-QCL flux measurements systems were determined to be 0.12 and 0.07 and 0.08 s, respectively. The main factors affecting the response time of the closed-path EC system are the damping of fluctuations in the sampling line and the instrumental response. Since the flow rate of CS-TDL system was higher, it can be concluded that the response characteristics of other two instruments are superior. The response time of the EC system including LGR-CW-QCL was larger due to the laminar tube flow regime, but the instrumental response was not determined based on the current field measurements.

Aerodyne AR-CW-QCL has the lowest detection limit due to its low noise level (around 0.12 ppb at 10 Hz sampling rate) compared to Los Gatos LGR-CW-QCL instrument (std of noise 0.60 ppb) and has therefore advantage in resolving low fluxes over short averaging periods. The noise level of AR-P-QCL was comparable to LGR-CW-QCL instrument but the old generation instrument Campbell CS-TDL suffered clearly from higher noise level (around 2 ppb). The flux detection limits due to instrumental noise for the observation conditions prevailing at the site were determined to be around 10^{-2} nmol m^{-2} s^{-1} for AR-CW-QCL, 4×10^{-2} nmol m^{-2} s^{-1} for LGR-CW-QCL and AR-P-QCL and 0.15 nmol m^{-2} s^{-1} for CS-TDL. Based on half-hour as well as long-term flux comparison, the best correspondence was observed between the systems with new generation instruments AR-CW-QCL and LGR-CW-QCL, of which the former has the advantage in detecting lower fluxes at half-hourly averaging basis (lower noise level).

BGD
11, 11747–11783, 2014

Acknowledgements. This work was supported by the Academy of Finland (project No. 118780 and 127456). ICOS (271878), ICOS-Finland (281255) and ICOS-ERIC (281250), DEFROST Nordic Centre of Excellence and InGOS EU are gratefully acknowledged for funding this work.

References

Aubinet, M., Grelle, A., Ibrom, A., Rannik, Ü., Moncrieff, J., Foken, T., Kowalski, A. S., Martin, P. H., Berbigier, P., Bernhofer, Ch., Clement, R., Elbers, J., Granier, A., Grünwald, T., Morgenstern, K., Pilegaard, K., Rebmann, C., Snijders, W., Valentini, R., and Vesala, T.: Estimates of the annual net carbon and water exchange of European forests: the EUROFLUX methodology, Adv. Ecol. Res., 30, 113–175, 2000.

Christensen, S., Ambus, P., Arah, J. R., Clayton, H., Galle, B., Griffith, D. W. T., Hargreaves, K. J., Klemedtsson, L., Lind, A. M., Maag, M., Scott, A., Skiba, U., Smith, K. A., Welling, M., and Wienhold, F. G.: Nitrous oxide emissions from an agricultural field: comparison between measurements by flux chamber and micrometeorological techniques, Atmos. Environ., 30, 4183–4190, 1996.

Eugster, W., Zeyer, K., Zeeman, M., Michna, P., Zingg, A., Buchmann, N., and Emmenegger, L.: Methodical study of nitrous oxide eddy covariance measurements using quantum cascade laser spectrometery over a Swiss forest, Biogeosciences, 4, 927–939, doi:10.5194/bg-4-927-2007, 2007.

Famulari, D., Nemitz, E., Di Marco, C., Phillips, G. J., Thomas, R., House, E., and Fowler, D.: Eddy-Covariance measurements of nitrous oxide fluxes above a city, Agr. Forest Meteorol., 150, 786–793, 2010.

FAO, World reference base for soil resources 2006: World Soil Resources Reports 103, Rome, Italy, 2006.

Finkelstein, P. L. and Sims, P. F.: Sampling error in eddy correlation flux measurements, J. Geophys. Res., 106, 3503–3509, 2001.

Finnigan, J. J., Clement, R., Malhi, Y., Leuning, R., and Cleugh, H. A.: A re-evaluation of longterm flux measurement techniques – Part I: Averaging and coordinate rotation, Bound.-Lay. Meteorol., 107, 1–48, 2003.

BGD
11, 11747–11783, 2014

Flechard, C., Neftel, A., Jocher, M., and Amman, C.: Bi-directional soil–atmosphere N_2O exchange over two mown grassland systems with contrasting management practices, Glob. Change Biol., 11, 2114–2127, 2005.
Foken, T. and Wichura, B.: Tools for quality assessment of surface-based flux measurements, Agr. Forest Meteorol., 78, 83–105, 1996.
Foken, T., Leuning, R., Oncley, S. R., Mauder, M., and Aubinet, M.: Corrections and Data Quality Control, in Eddy Covariance. A Practical Guide to Measurement and Data Analysis, Springer Science+Business Media B. V., 85–131, doi:10.1007/978-94-007-2351-1, 2012.
Horst, T. W.: A simple formula for attenuation of eddy fluxes measured with first-order-response scalar sensors, Bound.-Layer Meteorol., 82, 219–233, 1997.
Järvi, L., Nordbo, A., Rannik, Ü., Haapanala, S., Riikonen, A., Mammarella, I., Pihlatie, M., and Vesala, T.: Urban nitrous oxide fluxes measured using the eddy-covariance technique in Helsinki, Finland, Boreal Environm. Res., 19, in press, 2014.
Kaimal, J. C. and Finnigan, J. J.: Atmospheric Boundary Layer Flows, Their Structure and Measurement, Oxford University Press, New York, 1994.
Kaimal, J. C., Wyngaard, J. C., Izumi, Y., and Cotè, O. R.: Spectral characteristics of surface layer turbulence, Q. J. Roy. Meteor. Soc., 98, 563–589, 1972.
Korhonen, J. F. J., Pihlatie, M., Pumpanen, J., Aaltonen, H., Hari, P., Levula, J., Kieloaho, A.-J., Nikinmaa, E., Vesala, T., and Ilvesniemi, H.: Nitrogen balance of a boreal Scots pine forest, Biogeosciences, 10, 1083–1095, doi:10.5194/bg-10-1083-2013, 2013.
Kroon, P. S., Hensen, A., Jonker, H. J. J., Zahniser, M. S., van 't Veen, W. H., and Vermeulen, A. T.: Suitability of quantum cascade laser spectroscopy for CH_4 and N_2O eddy covariance flux measurements, Biogeosciences, 4, 715–728, doi:10.5194/bg-4-715-2007, 2007.
Laville, P., Henault, C., Renault, P., Cellier, P., Oriol, A., Devis, X., Flura, D., and Germon, J. C.: Field comparison of nitrous oxide emission measurements using micrometeorological and chamber methods, Agronomie, 17, 375–388, 1997.
Lee, B. H., Wood, E. C., Zahniser, M. S., McManus, J. B., Nelson, D. D., Herndon, S. C., Santoni, G. W., Wofsy, S. C., and Munger, J. W.: Simultaneous measurements of atmospheric HONO and NO_2 via absorption spectroscopy using tunable mid-infrared continuous-wave quantum cascade lasers, Appl. Phys. B, 102, 417–423, 2011.
Lenschow, D. H. and Kristensen, L.: Uncorrelated noise in turbulence measurements, J. Atmos. Ocean. Technol., 2, 68–81, 1985.

BGD
11, 11747–11783, 2014

Lenschow, D. H., Mann, J., and Kristensen, L.: How long is long enough when measuring fluxes and other turbulence statistics?, J. Atmos. Ocean. Technol., 18, 661–673, 1994.
Lenschow, D., Wulfmeyer, V., and Senff, C.: Measuring second- through fourth-order moments in noisy data, J. Atmos. Ocean. Technol., 17, 1330–1347, 2000.
Mammarella, I., Launiainen, S., Gronholm, T., Keronen, P., Pumpanen, J., Rannik, Ü., Vesala, T.: Relative humidity effect on the high frequency attenuation of water vapour flux measured by a closed-path eddy covariance system, J. Atmos. Ocean. Technol., 26, 1856–1866, 2009.
Mammarella, I., Werle, P., Pihlatie, M., Eugster, W., Haapanala, S., Kiese, R., Markkanen, T., Rannik, Ü., and Vesala, T.: A case study of eddy covariance flux of N_2O measured within forest ecosystems: quality control and flux error analysis, Biogeosciences, 7, 427–440, doi:10.5194/bg-7-427-2010, 2010.
Massman, W.: A simple method for estimating frequency response corrections for eddy covariance systems, Agr. Forest Meteorol., 104, 185–198, 2000.
Mauder, M., Cuntz, M., Druee, C., Graf, A., Rebmann, C., Schmid, H. P., Schmidt, M., and Steinbrecher, R.: A strategy for quality and uncertainty assessment of long-term eddy covariance measurements, Agr. Forest Meteorol., 169, 122–135, doi:10.1016/j.agrformet.2012.09.006, 2013.
McManus, J. B., Nelson, D. D., Shorter, J. H., Jiménez, R., Herndon, S., Saleska, S., and Zahniser, M. S.: A high precision pulsed QCL spectrometer for measurements of stable isotopes of carbon dioxide, J. Modern Optics, 52, 2309–2321, 2005.
Moncrieff, J. B., Massheder, J. M., de Bruin, H., Elbers, J., Friborg, T., Heusinkveld, B., Kabat, P., Scott, S., Soegaard, H., and Verhoef, A.: A system to measure surface fluxes of momentum, sensible heat, water vapour and carbon dioxide, J. Hydrol., 188–189, 589–611, 1997.
Moore, C. J.: Frequency response corrections for eddy correlation systems, Bound.-Lay. Meteorol., 37, 17–35, 1986.
Neftel, A., Flechard, C., Ammann, C., Conen, F., Emmenegger, L., and Zeyer, K.: Experimental assessment of N_2O background fluxes in grassland systems, Tellus B, 59, 470–482, 2007.
Nelson, D. D., Shorter, J. H., McManus, J. B., and Zahniser, M. S.: Sub-part-per-billion detection of nitric oxide in air using a thermoelectrically cooled mid-infrared quantum cascade laser spectrometer, Appl. Phys. B, 75, 343–350, 2002.
Pihlatie, M., Rinne, J., Ambus, P., Pilegaard, K., Dorsey, J. R., Rannik, Ü., Markkanen, T., Launiainen, S., and Vesala, T.: Nitrous oxide emissions from a beech forest floor measured by eddy

BGD
11, 11747–11783, 2014

covariance and soil enclosure techniques, Biogeosciences, 2, 377–387, doi:10.5194/bg-2-377-2005, 2005.
Pihlatie, M. K., Kiese, R., Brüggemann, N., Butterbach-Bahl, K., Kieloaho, A.-J., Laurila, T., Lohila, A., Mammarella, I., Minkkinen, K., Penttilä, T., Schönborn, J., and Vesala, T.: Greenhouse gas fluxes in a drained peatland forest during spring frost-thaw event, Biogeosciences, 7, 1715–1727, doi:10.5194/bg-7-1715-2010, 2010.
Pirinen, P., Simola, H., Aalto, J., Kaukoranta, J., Karlsson, P., and Ruuhela, R.: Tilastoja Suomen ilmastosta 1981–2010, Finnish Meteorological Institute, Helsinki, 2012.
Provencal, R., Gupta, M., Owano, T. G., Baer, D. S., Ricci, K. N., O'Keefe, A., and Podolske, J. R.: Cavity-enhanced quantum-cascade laser-based instrument for carbon monoxide measurements, Appl. Optics, 44, 6712–6717, 2005.
Rannik, Ü., Kolari, P., Vesala, T., and Hari, P.: Uncertainties in measurement and modelling of net ecosystem exchange of a forest ecosystem at different time scales, Agr. Forest Meteorol., 138, 244–257, 2006.
Rannik, Ü. and Vesala, T.: Autoregressive filtering versus linear detrending in estimation of fluxes by the eddy covariance method, Bound.-Lay. Meteorol., 91, 259–280, 1999.
Scanlon, T. M. and Kiely, G.: Ecosystem-scale measurements of nitrous oxide fluxes for an intensely grazed, fertilized grassland, Geophys. Res. Lett., 30, 1852, doi:10.1029/2003GL017454, 2003.
Schotanus, P., Nieuwstadt, F. T. M., and Debruin, H. A. R.: Temperature-measurement with a sonic anemometer and its application to heat and moisture fluxes, Bound.-Lay. Meteorol., 26, 81–93, 1983.
Smith, K. A., Clayton, H., Arah, J. R. M., Christensen, S., Ambus, P., Fowler, D., Hargreaves, K. J., Skiba, U., Harris, G. W., Wienhold, F. G., Klemedtsson, L., and Galle, B.: Micrometeorological and chamber methods for measurement of nitrous oxide fluxes between soils and the atmosphere: overview and conclusions, J. Geophys. Res., 99, D8 16541–16548, 1994.
Vickers, D. and Mahrt, L.: Quality control and flux sampling problems for tower and aircraft data, J. Atmos. Ocean. Tech., 14, 512–526, 1997.
Wang, K, Zheng, X., Pihlatie, M., Vesala, T., Liu, C., Haapanala, S., Mammarella, I., Rannik, Ü., Liu, H.: Comparison between static chamber and tunable diode laser-based eddy covariance techniques for measuring nitrous oxide fluxes from a cotton field, Agr. Forest Meteorol., 171–172, 9–19, 2013.

BGD
11, 11747–11783, 2014

Werle, P., Muecke, R., and Slemr, F.: The limits of signal averaging in atmospheric trace gas monitoring by tunable diode-laser absorption spectroscopy, Appl. Phys. B 57, 131–139, 1993.

Wienhold, F. G., Frahm, H., and Harris, G. W.: Measurements of N_2O fluxes from fertilized grassland using a fast response tunable diode laser spectrometer, J. Geophys. Res., 99, 16557–16567, 1994.

Zahniser, M. S., Nelson, D. D., McManus, J. B., Hern-don, S. C., Wood, E. C., Shorter, J. H., Lee, B. H., Santoni, G. W., Jimenez, R., Daube, B. C., Park, S., Kort, E. A., and Wofsy, S. C.: Infrared QC laser applications to field measurements of atmospheric trace gas sources and sinks in environmental research: enhanced capabilities using continuous wave QCLs, Proc. SPIE, 7222, doi:10.1117/12.815172, 2009.

BGD
11, 11747–11783, 2014

Table 1. Instrumental characteristics. Experimental precision values are based on flux measurements during the period DOY 206–271 (period II). TDL – Tunable Diode Laser; CW-QCL – Continuous-Wave Quantum Cascade Laser; P-QCL – Pulsed QCL.

Instrument model	TGA100A	CW-TILDAS-CS	N2O/CO-23d	QC-TILDAS-76-CS
Manufacturer	Campbell Scientific Inc.	Aerodyne Research Inc.	Los Gatos Research Inc.	Aerodyne Research Inc.
Acronym used in current study	CS-TDL	AR-CW-QCL	LGR-CW-QCL	AR-P-QCL
Measured species	N_2O	N_2O, H_2O, CO	N_2O, H_2O, CO	N_2O, CO_2, H_2O
Sample cell volume (ml)	480	500		500 (76 m path length)
Sample cell pressure (hPa)	50	53	117	53
Spectroscopic correction coefficient *b*	0.00 (drier used in sampling line)	0.39	0.00 (built-in correction by the instrument)	0.0235
Precision, 10 Hz noise std, $P_{10}/P_{50}/P_{90}$ this study (ppb)	1.89/1.98/2.1	0.12/0.12/0.14	0.46/0.60/0.78	0.43/0.46/0.51

BGD
11, 11747–11783, 2014

Table 2. Eddy covariance measurements setup, flux calculation and quality screening parameters.

Instrument	CS-TDL	AR-CW-QCL	LGR-CW-QCL	AR-P-QCL
Sampling height (m)	2.2/2.4	2.2/2.4	2.4	2.0/2.5
Horizontal separation[1] (m)	0.05	0.05	0.07	0.1
Tube inner diameter (mm)	4	4	8	4
Tube length (m)	17.8	16	16	8.5
Flow rate (LPM)	17	13.2	11.6	13.5
Lag time from tube flow (s)	0.79	0.91	4.2	0.48
Lag time window used in flux calculation (s)	1.0 ± 0.0	1.0 ± 0.0	1.0 ± 0.0[2]	1.0 ± 0.8[3]
Time constant used in spectral corrections (s)	0.12	0.07	0.26	0.15

[1] Refers to separation of the sampling inlet from the center position of the sonic anemometer. Vertical separation was 0.1 m for all instruments.
[2] Prior to flux calculation concentration records of LGR-CW-QCL were syncronised with AR-CW-QCL outputs.
[3] The lag time window was used to determine the lag time for CO_2, which was assigned as the lag time for N_2O.

BGD
11, 11747–11783, 2014

Table 3. Statistics of spectral corrections of fluxes as % of raw uncorrected fluxes: lower percentile/median/upper percentile. Based on flux measurements during the period DOY 206–271 (period II) and data classified as qualified (Table 4). Day time was defined by the elevation of sun higher than zero and night time lower than zero, respectively. Statistics were derived for data when measurements were available for all four instruments.

	CS-TDL	AR-CW-QCL	LGR-CW-QCL	AR-P-QCL
All data	4.0/6.2/10.2	2.4/3.6/6.0	6.9/12.3/20.0	4.5/7.3/14.8
Daytime data	4.0/6.1/9.8	2.6/3.6/5.8	6.9/12.0/18.5	4.5/6.9/10.5
Night data	3.6/6.3/11.3	2.2/3.6/6.4	6.7/12.9/22.3	4.5/7.7/20.2

BGD
11, 11747–11783, 2014

Table 4. Average fluxes (nmol m^{-2} s^{-1}) ±random error of the average. Period I DOY 110–181 (20 April–30 June 2011), Period II DOY 206–271 (25 July–28 September 2011), Period III DOY 272–324 (29 September–20 November 2011). % data available represents the fraction of half-hour periods when data from all 3 (or 4) instruments was available (data from wind direction interval 50–110° excluded), relative to full time period length. Averaging of fluxes for each instrument was performed only for data if measurements were available for all instruments used in respective period. No gap filling was used.

	% data available	% data qualified (out of available)	# 30 min periods averaged	CS-TDL	AR-CW-QCL	LGR-CW-QCL	AR-P-QCL
Period I	69.2	75.2	1797	0.931 ±0.018	0.870 ±0.009		0.560 ±0.011
Period II	55.0	79.4	1383	0.183 ±0.010	0.146 ±0.006	0.138 ±0.007	0.124 ±0.003
Period III	61.4	78.2	1220		0.067 ±0.002	0.057 ±0.002	0.058 ±0.003

BGD
11, 11747–11783, 2014

Table 5. Average micrometeorological conditions during the experimental periods. Period I DOY 110–181 (20 April–30 June 2011), Period II DOY 206–271 (25 July–28 September 2011), Period III DOY 272–324 (29 September–20 November 2011). Day time was defined by the elevation of sun higher than zero and night time lower than zero, respectively. Average latent heat fluxes were determined from IRGA measurements.

	Temperature	Air rel. humidity, %	Wind speed, $m\,s^{-1}$	Friction velocity, $m\,s^{-1}$	Sensible heat flux, $W\,m^{-2}$	Latent heat flux, $W\,m^{-2}$
Day, I	11.6	62.9	2.21	0.28	27.5	78.9
Night, I	6.5	78.3	1.34	0.14	−20.2	8.1
Day, II	15.3	75.2	1.35	0.26	9.7	109.3
Night, II	11.2	90.3	1.06	0.17	−18.6	10.1
Day, III	6.1	85.0	1.46	0.29	−10.8	41.5
Night, III	4.8	90.6	1.21	0.23	−23.5	11.5

BGD
11, 11747–11783, 2014

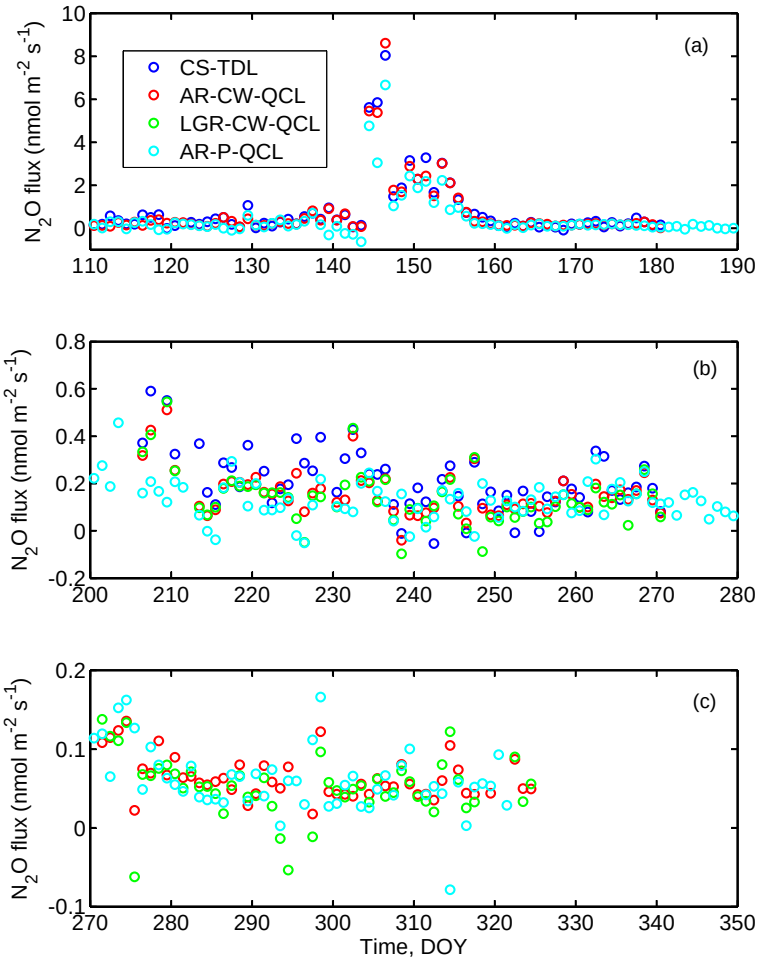

Figure 1. Daily average fluxes for four instruments. No gap-filling was used in calculation of daily average fluxes.

BGD
11, 11747–11783, 2014

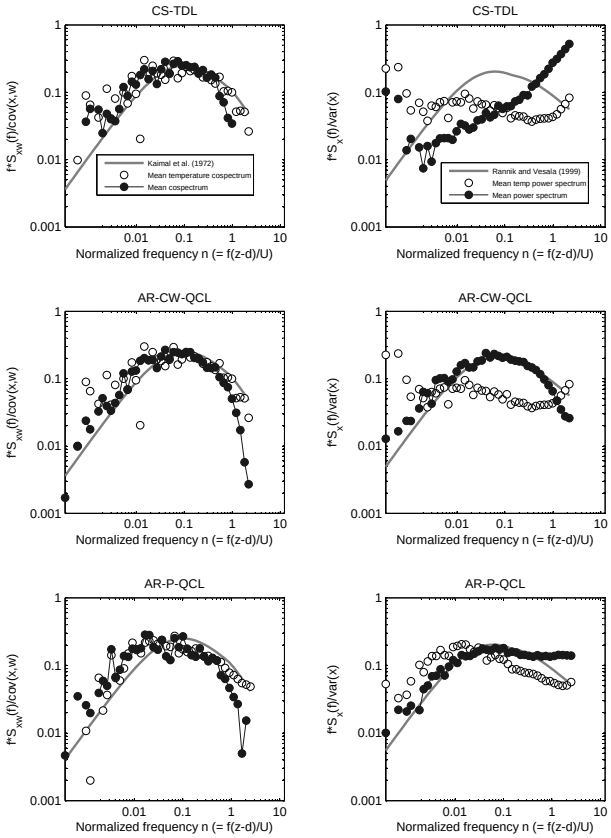

Figure 2. Normalised co-spectra (left panels) and spectra (right panels) of N_2O measurements by instruments CS-TDL (upper panels), AR-CW-QCL (middle panels) and AR-P-QCL (lower panels) during the high flux period, DOY 146 (26 May 2011) 7:00 to 13:00 EET. The RCG crop was about 0.4 m tall during the given period.

BGD
11, 11747–11783, 2014

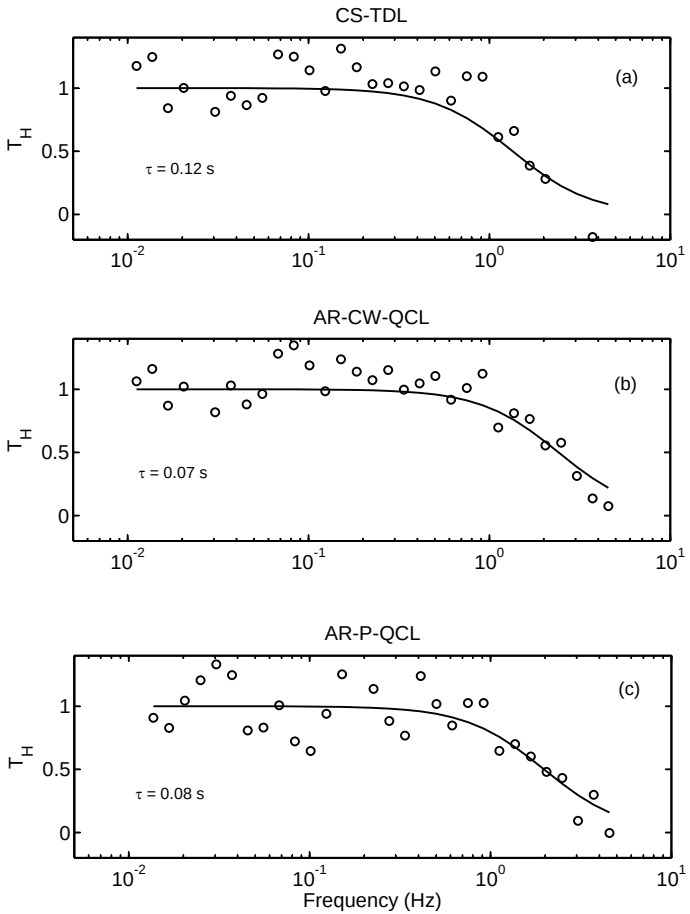

Figure 3. Co-spectral transfer functions derived for CS-TDL **(a)**, AR-CW-QCL **(b)** and AR-P-QCL **(c)** from the temperature and N_2O co-spectra presented in Fig. 2.

BGD
11, 11747–11783, 2014

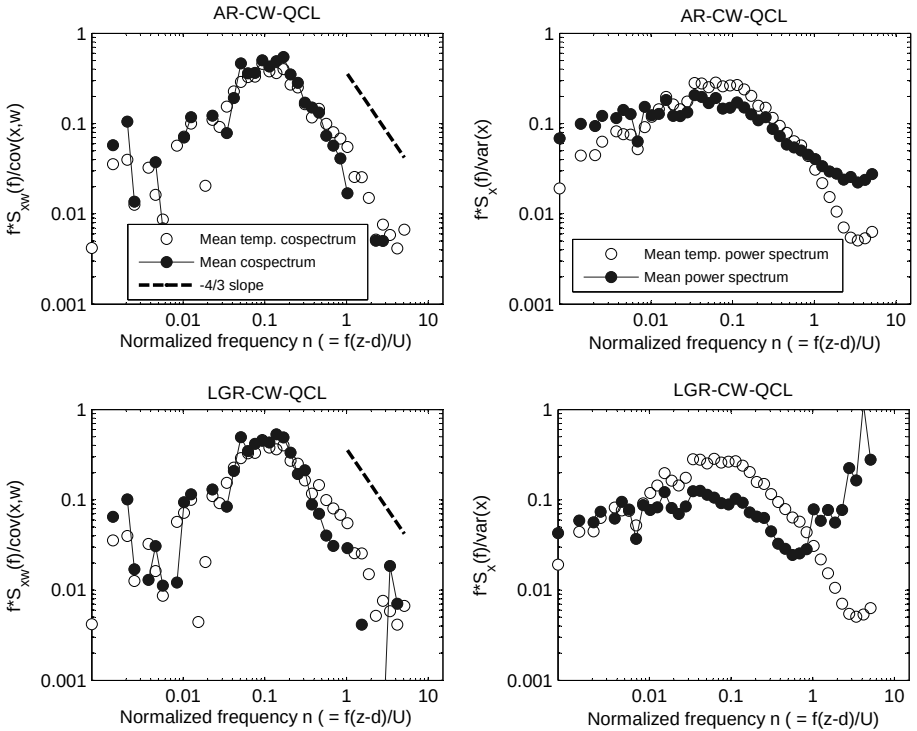

Figure 4. Normalised co-spectra (left panels) and spectra (right panels) of N_2O measurements by instruments AR-CW-QCL (upper panels) and LGR-CW-QCL (lower panels) during the period DOY 216 (04 August 2011) 00:30 to 4:00 EET. The RCG crop was about 1.8 m tall during the given period.

BGD
11, 11747–11783, 2014

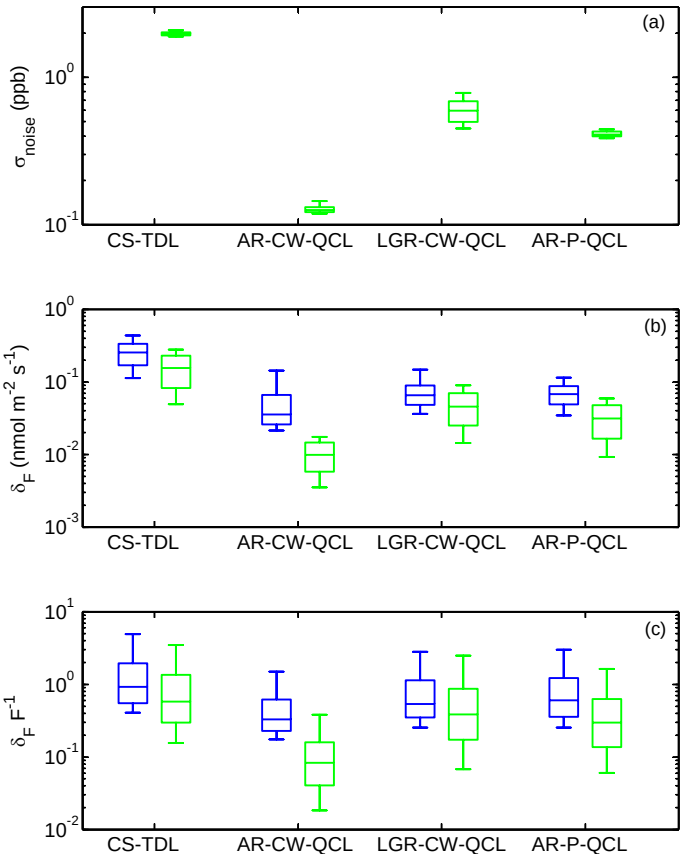

Figure 5. (a) Instrumental noise, presented as one standard deviation of the noise at 10 Hz frequency, **(b)** N_2O flux random error (blue) and flux random error due to instrumental noise (green) statistics; **(c)** the same as **(b)** but for relative fluxes. The boxplots present the lower and upper percentiles, quartiles and median values of the distributions. Based on flux measurements during the period DOY 206–271 (period II).

BGD
11, 11747–11783, 2014

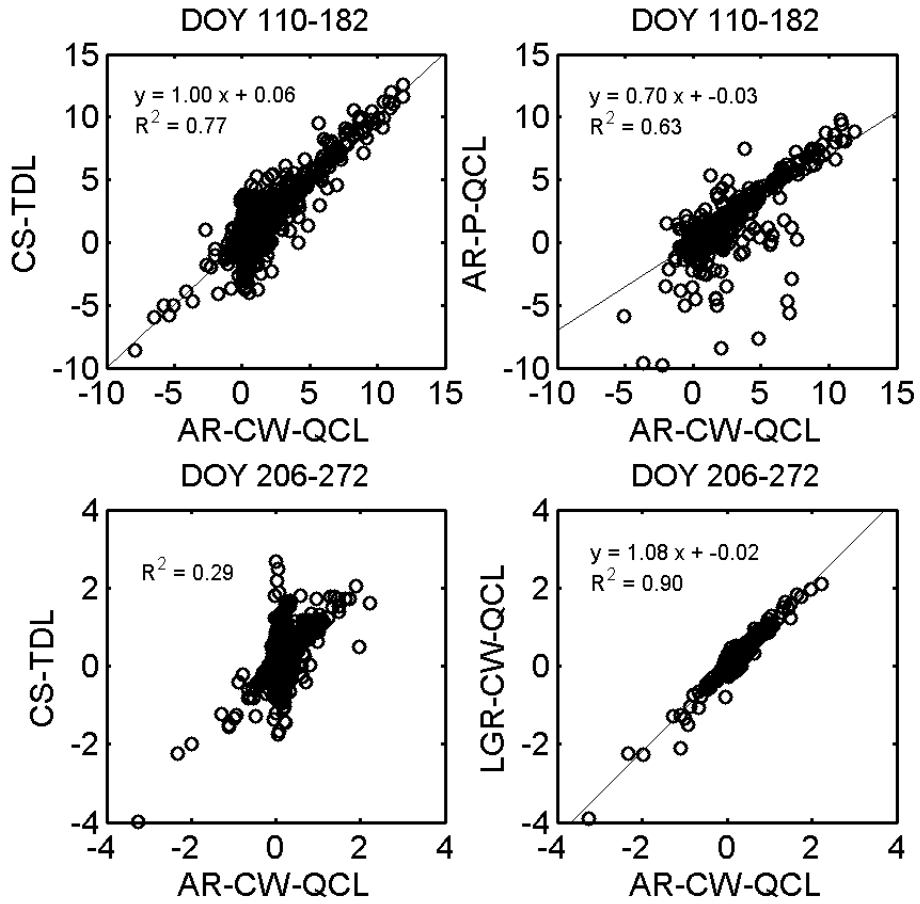

Figure 6. Correlation scatter plots of 30 min average N_2O fluxes (in nmol m^{-2} s^{-1}), as measured by CS-TDL and AR-P-QCL vs. AR-CW-QCL during the period I DOY 110–181 (upper panels), and CS-TDL and LGR-CW-QCL vs. AR-CW-QCL during the period II DOY 206–271 (lower panels). The lines present the linear fit with coefficients presented on the plots.

BGD
11, 11747–11783, 2014

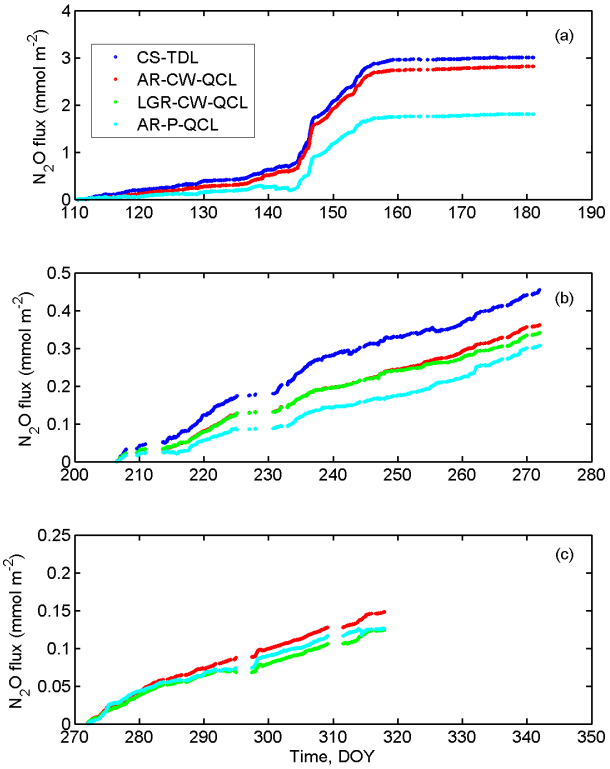

Figure 7. Cumulative sums of available flux data for three periods: upper panel **(a)** period I DOY 110–181 (20 April–30 June 2011), middle panel **(b)** period II DOY 206–271 (25 July–28 September 2011), lower panel **(c)** period III DOY 272–324 (29 September–20 November 2011). Accumulation of fluxes for each instrument was performed only for data if measurements were available for all instruments used in respective period. No gap filling was used.

BGD
11, 11747–11783, 2014